Size effects in friction of multiatomic sliding contacts

Masanori Igarashi and Akiko Natori*
Department of Electronic-Engineering, The University of Electro-Communications (UEC–Tokyo), 1-5-1 Chofugaoka, Chofu, Tokyo 182-8585, Japan

Jun Nakamura†
Department of Electronic-Engineering, The University of Electro-Communications (UEC–Tokyo), 1-5-1 Chofugaoka, Chofu, Tokyo 182-8585, Japan
and The Institute for Solid State Physics, The University of Tokyo, 5-1-5 Kashiwa-no-ha, Kashiwa, Chiba 277-8581, Japan
(Received 4 April 2008; revised manuscript received 29 July 2008; published 28 October 2008)

We studied the multiatomic contact effect of a friction force microscope at a finite temperature using the dynamical simulation of the Frenkel-Kontrova-Tomlinson model with a finite contact size. The friction force depends crucially on both the lattice mismatch between the tip of a friction force microscope and the sample surface and the strength of the lateral coupling between atoms in the tips. In the case of strong coupling, the friction force depends strongly on both the lattice mismatch and the tip size: there exists a magic size at which the friction force is reduced dramatically due to suppression of the effective corrugation of the surface potential to drag the tip. In the case of weak coupling, a decrease of the friction force with increasing temperature is enhanced as the tip size increases, irrespective of the lattice mismatch. This is caused by the enhanced thermal fluctuation for the multiatomic contact. The correlation among atoms in the multiatomic contact is also discussed.

DOI: 10.1103/PhysRevB.78.165427 PACS number(s): 68.35.Af, 07.79.Sp, 81.40.Pq, 46.55.+d

I. INTRODUCTION

Scientists and engineers have long been intrigued by the phenomena of friction and a friction force microscope (FFM) was developed as a new ideal experimental method to detect friction in the atomic scale. Mate *et al.*[1] reported the first observation of a stick-slip movement of the tip with the atomic periodicity of the sample surface structure. Recently, atomic scale control of friction has also been tried by actuation of nanometer-sized contacts.[2]

A number of experimental results obtained by a friction force microscope have been explained successfully by a Tomlinson model[3] in which a single spring and a single-atomic tip are assumed. The cantilever and the contact of the FFM are thought to act as springs in series and this picture gives the single-spring model with the effective spring constant. The occurrence of the stick slip as a function of load[4,5] and the occurrence of slip over multiple lattice units[1,6–10] have been analyzed satisfactorily. Furthermore, the scanning velocity dependence of the atomic friction have also been elucidated by including thermal activation of the slip motion[9,11,12] for the sliding velocity of not so high. As for the observed nonmonotonic dependence of the friction force in high sliding velocities,[4] two mechanisms have been proposed: (1) the energy dissipation mainly in a tip but a substrate[13,14] and (2) occurrence of higher slips at high sliding velocities.[15]

Recently, the "extended Tomlinson model" has been proposed by Maier *et al.*:[16] a two-spring model where one spring represents a cantilever and the other spring a microscopic contact separately and a multitip model of multiatomic contact with the surface. The microscopic contact spring originates from the tangential displacement between atomic layers of a tip apex.[17] Maier *et al.*[16] showed with the two-spring model that the thermal fluctuation of the friction force clearly followed the frequency of the cantilever resonance. In the two-spring model, a new nontrivial regime has also been expected if the jump frequency of a tip is larger than or equal to the characteristic frequency of the cantilever.[17] However, the two-spring model can be reduced to the single-spring model in the opposite limit of the jump frequency of the tip much less than the characteristic frequency of the cantilever.[17] As for the multiatomic contact effect, Maier *et al.*[16] pointed out that the number of atoms was crucial to interpret the duration of the slip: the slips become slower with the increasing number of atoms. In the multiatomic contact model proposed by Maier *et al.*, however, the coupling between atoms is not considered. The atomic interaction within the same atomic layers of a tip apex is thought to cause the coupling between atoms.

The coupling between atoms in the multiatomic contact can be considered in the Frenkel-Kontrova model.[18,19] In the Frenkel-Kontrova model, an adsorbed monolayer on an atomically flat surface is modeled: adsorbate atoms are coupled with springs and they interact with a spatially periodic surface potential. The Frenkel-Kontrova-Tomlinson model is constituted by combining the Frenkel-Kontrova model with the Tomlinson model. In the Frenkel-Kontrova-Tomlinson model, Weiss and Elmer[20,21] studied both the static and the kinetic frictions in the limit of zero temperature. In these studies, the periodic boundary condition was used for atoms in contact with the surface and the size effect of the contact has not been studied. In our previous paper,[22] on the other hand, we studied the size effect on the activation energy of the diffusion coefficient of the cluster using the Frenkel-Kontrova model with a finite contact size and clarified the condition of occurrence of the magic size where the activation energy can be reduced dramatically. Krylov[23] showed that a dynamical misfit caused by the thermal vibrations of the cluster atoms leads to a dramatic increase of the

pre-exponential factor in the diffusion coefficient, in the case of weak corrugation of the surface potential compared to the coupling between atoms.

Our aim is to clarify the size effect for multiatomic contacts on the atomistic friction mechanism of a friction force microscope at a finite temperature for low sliding velocities. We used the Frenkel-Kontrova-Tomlinson model with a finite contact size to take into account the coupling between atoms. Ermak's algorithm[24] is used to solve numerically the Langevin equation for each atom in contact with the surface. We address the dependence of the friction on the number of atoms in contact with the surface, the lattice mismatch between the tip and the surface, the stiffness of the contact atomic layer, and the temperature.

II. FORMULATION

In the one-dimensional "extended Tomlinson model" (Ref. 16) of a tip apex with N atoms with a single effective spring, the total interaction energy is written as

$$E_e(x,R) = -\sum_{i=1}^{N} U_1 \cos\left(\frac{2\pi x_i}{a}\right) + \sum_{i=1}^{N} \frac{k_1}{2}(x_{0i} - x_i)^2, \quad (1)$$

where x_i is a coordinate of each atom within the atomic layer in contact with the sample surface and x_{0i} is the equilibrium position of each atom where the springs with k_1 have no deviations at the support point of the FFM. Hence, x_{0i} can be written as $x_{0i}=R+(\frac{N+1}{2}-i)b$. Here, b is the equilibrium separation, i.e., the lateral lattice constant of the tip apex, and R is the position of the support. x represents the full set of x_i for $i=1,2,\ldots,N$. The first term of Eq. (1) is the periodic potential of a substrate with a lattice constant a and the second term is the effective elastic interaction with an elastic constant k_1 between the tip atom and the support point. The parameters for each N-tip simulation were assumed[16] with each of the contact springs having the tip stiffness of $k_1 = k_{\mathrm{tip}}/N$, the amplitude of the potential corrugation of $U_1 = U/N$, and the mass of the tip $m=m_{\mathrm{tip}}/N$. Here, k_{tip}, U, and m_{tip} are the total elastic constant, the amplitude of the potential corrugation, and the total mass of the tip, respectively. This scaling was chosen in order to always reproduce the experimentally observed slope and amplitude of the stick-slip force curves at $T=0$ for a different number of atoms involved. In Eq. (1), the coupling between atoms is completely neglected. We consider the interaction as an elastic interaction with the spring constant k_2 between neighboring atoms and modified the total interaction energy as follows:

$$E_m(x,R) = E_e(x,R) + \sum_{i=1}^{N-1} \frac{k_2}{2}(x_i - x_{i+1})^2. \quad (2)$$

It should be mentioned that our modified multiatomic contact model is equivalent to the Frenkel-Kontrova-Tomlinson model with a finite contact size and can be reduced to the "extended Tomlinson model" (Ref. 16) with a single spring in the case of $k_2=0$. Furthermore, it reproduces the results in a single-atomic tip model with k_{tip}, U, and m_{tip}, in the rigid commensurate case of $k_2=\infty$ and $a=b$, irrespective of the number of N. In a conventional single-tip model, the stick-slip motion of a tip atom does not occur for $k_{\mathrm{tip}}a^2/U > (2\pi)^2$, while the stick slip is induced for $(2\pi)^2 > k_{\mathrm{tip}}a^2/U$. This criterion changes dramatically in a multiatomic contact model with a lattice mismatch between a and b. In the case of $k_2=\infty$, the effective amplitude U' of the corrugation of the total potential of the substrate to drag a tip is calculated as[22]

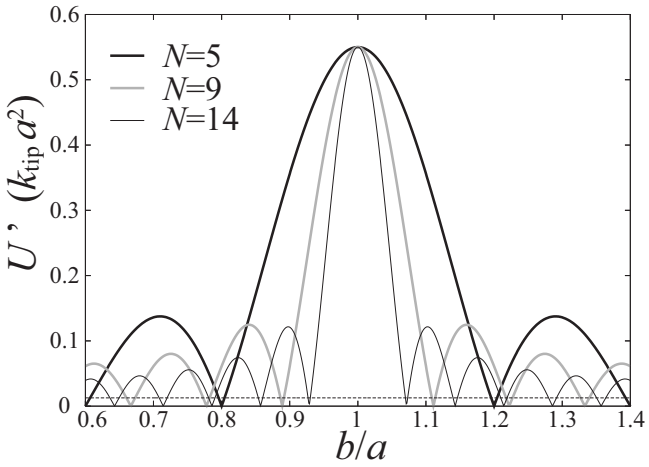

FIG. 1. The relation between the effective amplitude U' of the corrugation and the lattice mismatch b/a at three values of N. The horizontal line represents the threshold of $U'=k_{\mathrm{tip}}a^2/(2\pi)^2$ for occurrence of the stick-slip motion. Here, $U=0.55k_{\mathrm{tip}}a^2$ is assumed.

$$U' = \frac{U|\sin(\pi bN/a)|}{N|\sin(\pi b/a)|}. \quad (3)$$

The behavior of U' as a function of b/a is plotted for some values of N in Fig. 1, with the threshold of the stick-slip motion. It is seen that U' vanishes if the lattice mismatch satisfies the relation of $bN=an$ for integer n. This means that there may exist a magic size N at which the effective potential corrugation vanishes.

When the support point R is scanned at a finite velocity v, the dynamics of each tip atom is described by the Langevin equation[8,12]

$$m\ddot{x}_i + m\mu\dot{x}_i = -\frac{\partial E_m(x,vt)}{\partial x_i} + f_i, \quad (4)$$

where m is the mass of m_{tip}/N, μ is the viscous friction coefficient representing the single-particle energy exchange with a substrate, and E_m is the total interaction energy given by Eq. (2), where R is set as $R=vt$. μ determines the momentum relaxation time and is assumed to be independent of N to reproduce a single tip model in the case of $k_2=\infty$ and $a=b$. Here, f_i is a random force that is related to the viscous friction coefficient μ by the fluctuation dissipation theorem

$$\langle f_i(t) f_i(t') \rangle = 2\mu m k_B T \delta(t-t'), \quad (5)$$

where k_B is the Boltzmann constant and T is an absolute temperature. We used Ermak's algorithm[24] to solve the Langevin equation numerically. The friction force F can be calculated as

$$F = k_{\mathrm{tip}}(vt - x_G), \tag{6}$$

where x_G is the position of the center of mass $x_G = \Sigma_{i=1}^{N} x_i/N$.

In numerical calculation, we take a as a unit of length, m_{tip} as a unit of mass, and $k_{\mathrm{tip}}a^2$ as a unit of energy. This means that the unit of time is $\sqrt{m_{\mathrm{tip}}/k_{\mathrm{tip}}}$. In this unit system, our model is characterized by four dimensionless parameters: a viscous friction coefficient $\mu\sqrt{m_{\mathrm{tip}}/k_{\mathrm{tip}}}$, an amplitude of the potential corrugation $U/k_{\mathrm{tip}}a^2$, a scanning velocity of a support point of the FFM $v\sqrt{m_{\mathrm{tip}}/k_{\mathrm{tip}}}/a$, and a temperature $Tk_B/k_{\mathrm{tip}}a^2$. For example, the following values were assumed by Riedo *et al.*[4] and Reimann and Evstigneev:[13] $a = 0.52$ nm, $k_{\mathrm{tip}} = 1.2$ N/m, $U \simeq 1.1$ eV, $m_{\mathrm{tip}} = 3 \times 10^{-12}$ kg, $\mu m_{\mathrm{tip}} = 0.8 \times 10^{-5}$ kg/s, and $v = 0.328$ μm/s. The corresponding dimensionless values are $v = 0.001$, $\mu = 4.2$, $U = 0.55$, and $k_BT = 0.013$ at room temperature. We adopted these dimensionless values in the following numerical calculation.

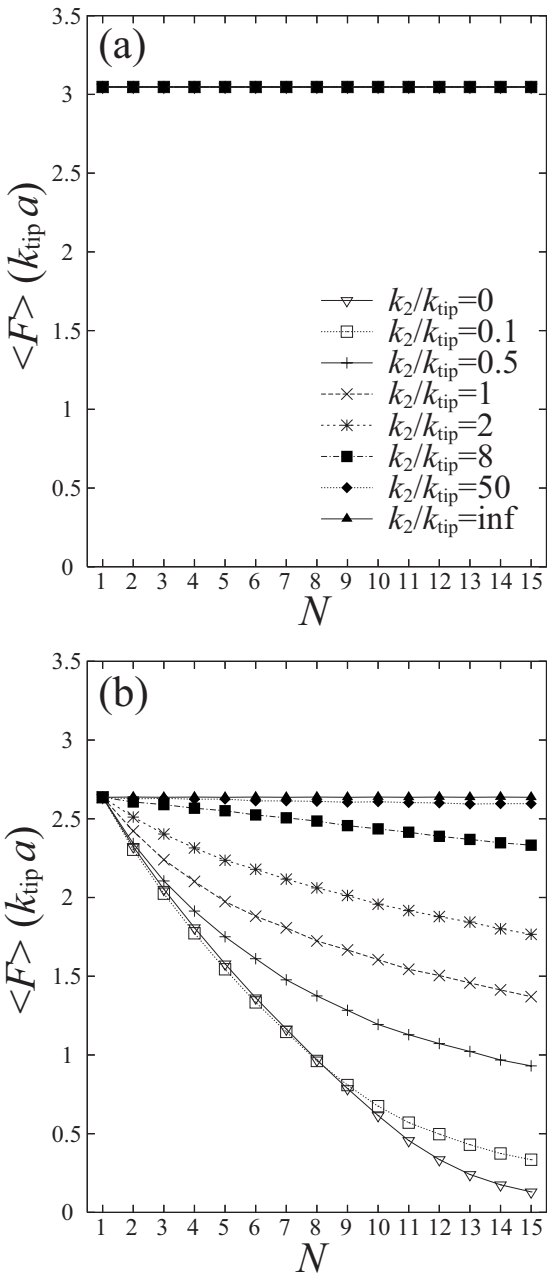

FIG. 2. The relation between the time-averaged friction force $\langle F \rangle$ and the tip size N in the lattice-matched case of $a=b$ for several values of k_2/k_{tip} at (a) $T=0$ and (b) $T=0.013k_{\mathrm{tip}}a^2/k_B$.

III. NUMERICAL RESULTS

At first, we present the results in the lattice-matched case of $a=b$ and elucidate the contact size dependence for several values of k_2/k_{tip}. In Fig. 2, the time-averaged friction force $\langle F \rangle$ is plotted as a function of the contact size N for several

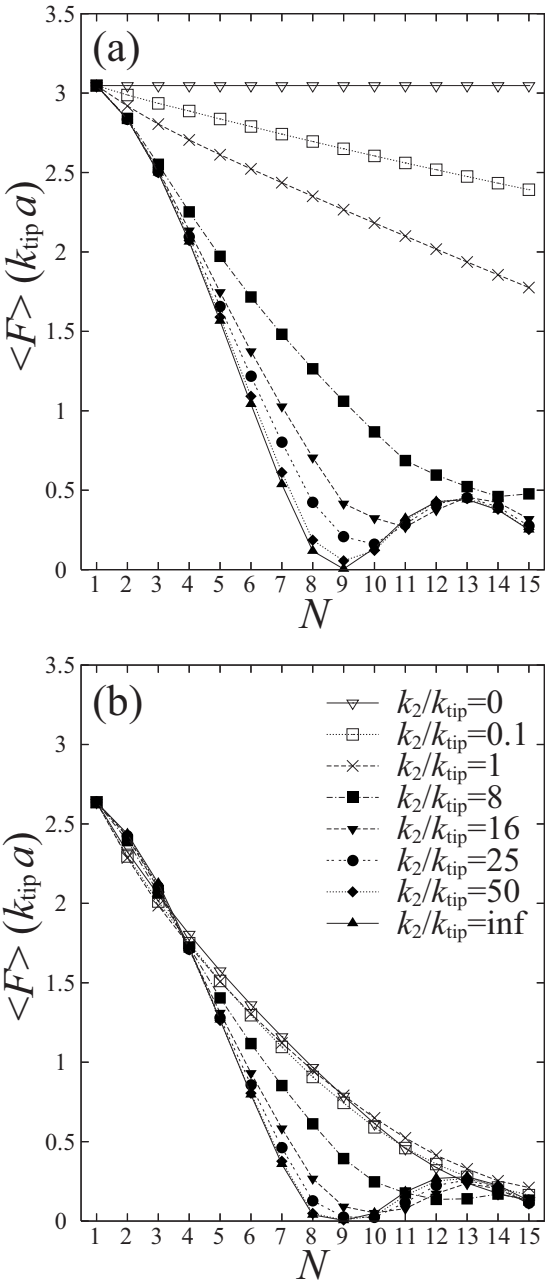

FIG. 3. The relation between the time-averaged friction force $\langle F \rangle$ and the tip size N in the lattice-mismatched case of $b/a = 0.887$ for several values of k_2/k_{tip} at (a) $T=0$ and (b) $T=0.013k_{\mathrm{tip}}a^2/k_B$.

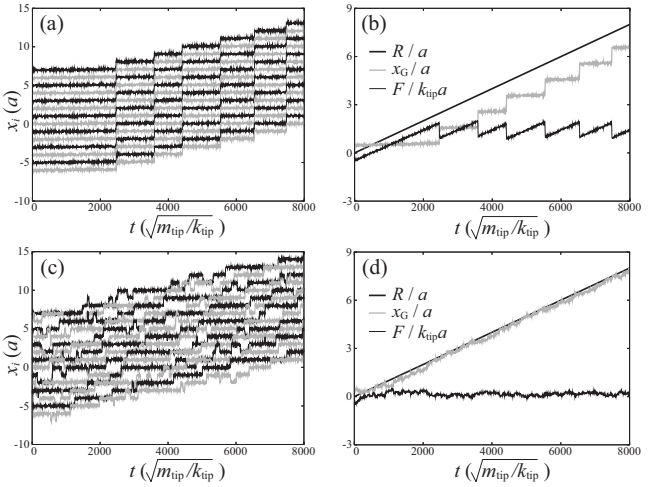

FIG. 4. The time t dependence of x_i for $1 \leq i \leq 14$, x_G, and F with $R=vt$ for (a),(b) $k_2/k_{\mathrm{tip}}=1$, and (c),(d) $k_2=0$, respectively. Here, $N=14$, $b/a=1$, and $T=0.013k_{\mathrm{tip}}a^2/k_B$.

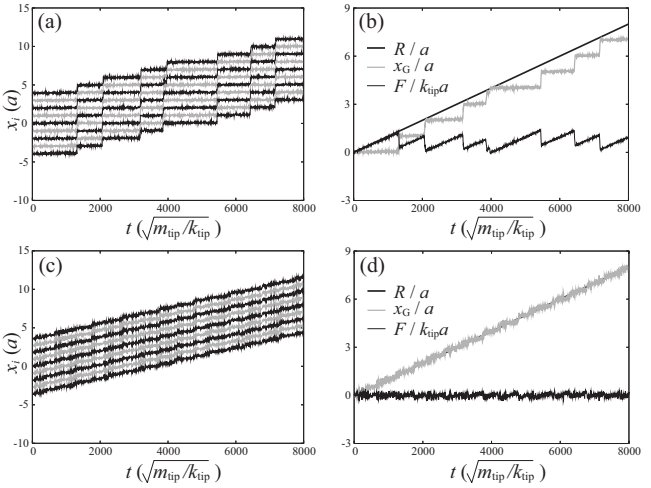

FIG. 5. The time t dependence of x_i for $1 \leq i \leq 9$, x_G, and F with $R=vt$ for (a),(b) $k_2/k_{\mathrm{tip}}=1$, and (c),(d) $k_2/k_{\mathrm{tip}}=50$, respectively. Here, $N=9$, $b/a=0.887$, and $T=0.013k_{\mathrm{tip}}a^2/k_B$.

values of k_2/k_{tip} at $T=0$ and at room temperature of $T=0.013$. $\langle F \rangle$ does not depend on both N and k_2/k_{tip} at $T=0$, while it depends on them at room temperature. In the case of $k_2=\infty$ which results in the single-atomic contact, the averaged friction force is reduced slightly at room temperature irrespective of the tip size N in Fig. 2(b). In the opposite extreme case of $k_2=0$ in Fig. 2(b), the averaged friction force is reduced remarkably with increasing the tip size N at room temperature. For the intermediate values of k_2, the averaged friction force takes the mean behavior between these two extreme cases. When there exists a lattice mismatch, on the other hand, the situation is changed dramatically. In Fig. 3, the time-averaged friction force $\langle F \rangle$ is plotted at the lattice mismatch of $b/a=0.887$ as a function of the tip size N for

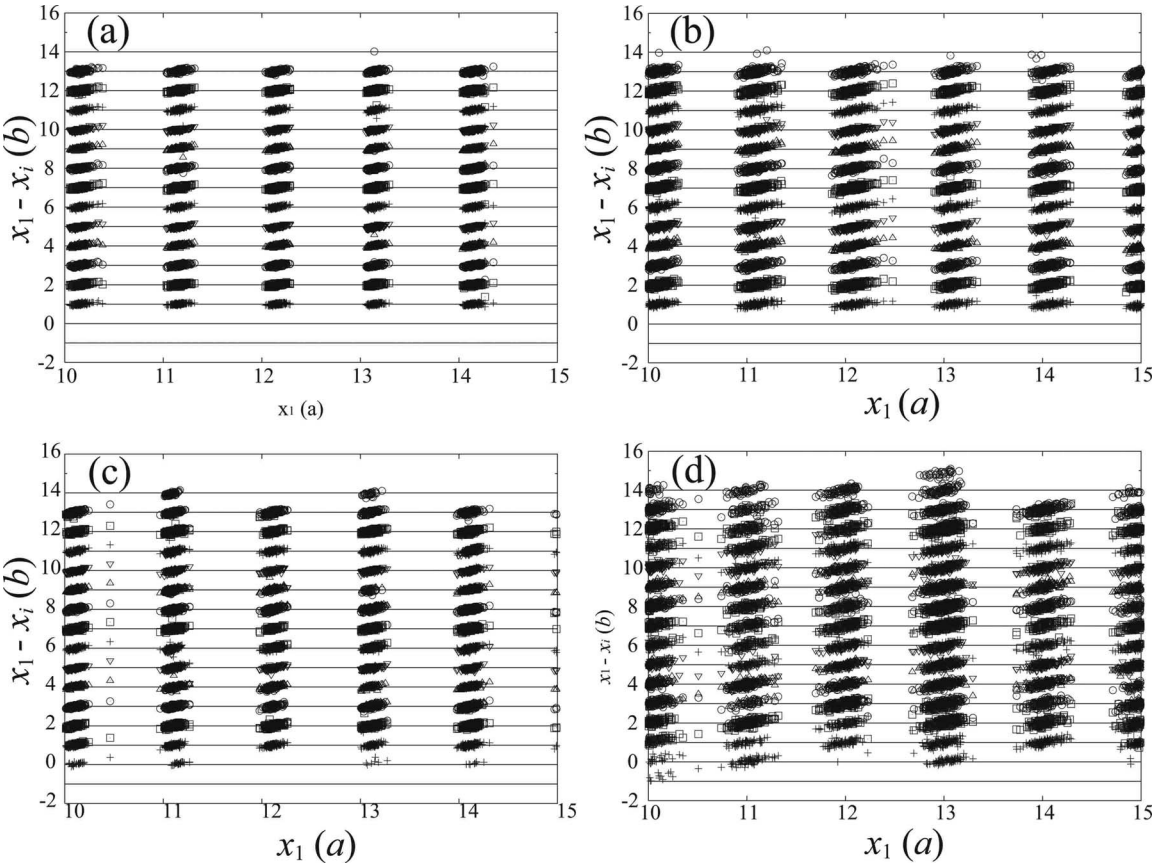

FIG. 6. (x_1-x_i) as a function of x_1 at $N=14$ for $b/a=1$. (a) $k_2/k_{\mathrm{tip}}=1$, $T=0.0026k_{\mathrm{tip}}a^2/k_B$, (b) $k_2/k_{\mathrm{tip}}=1$, $T=0.013k_{\mathrm{tip}}a^2/k_B$, (c) $k_2/k_{\mathrm{tip}}=0$, $T=0.0026k_{\mathrm{tip}}a^2/k_B$, and (d) $k_2/k_{\mathrm{tip}}=0$, $T=0.013k_{\mathrm{tip}}a^2/k_B$.

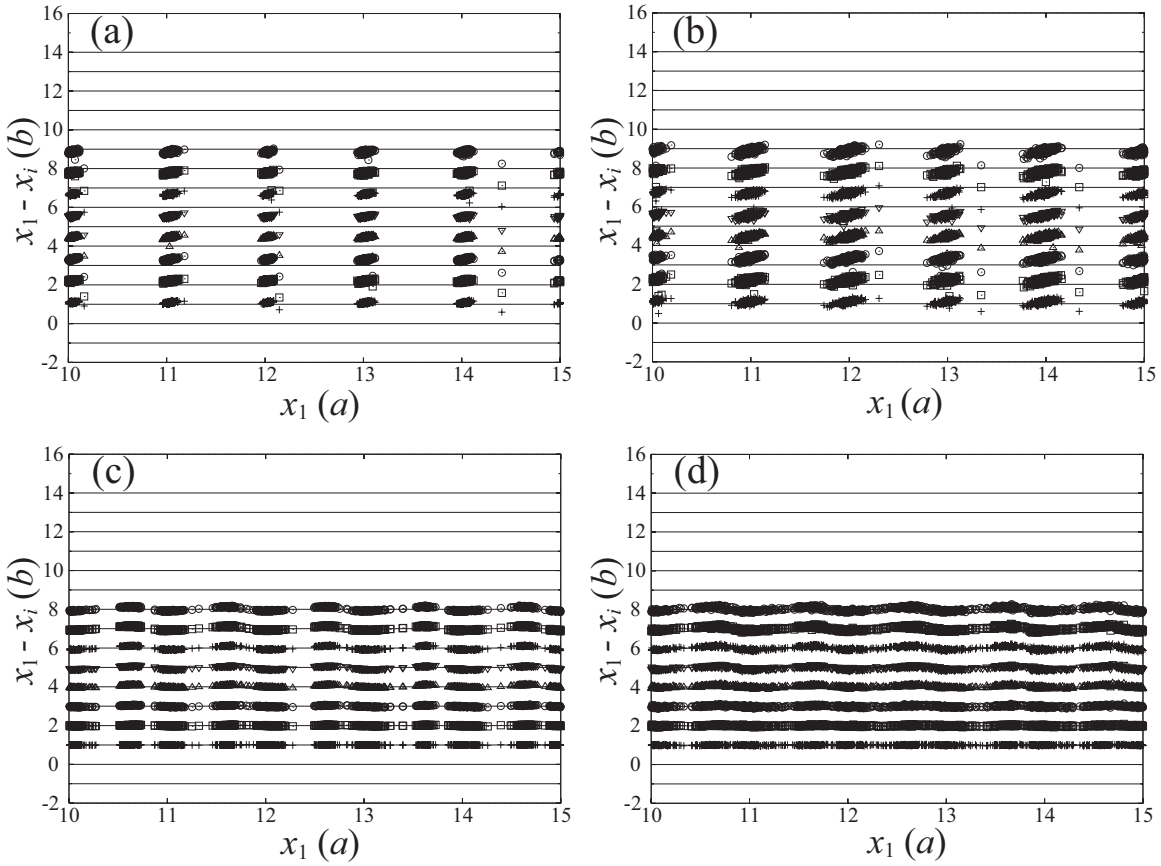

FIG. 7. (x_1-x_i) as a function of x_1 at $N=9$ for $b/a=0.887$. (a) $k_2/k_{\mathrm{tip}}=1$, $T=0.0026k_{\mathrm{tip}}a^2/k_B$, (b) $k_2/k_{\mathrm{tip}}=1$, $T=0.013k_{\mathrm{tip}}a^2/k_B$, (c) $k_2/k_{\mathrm{tip}}=50$, $T=0.0026k_{\mathrm{tip}}a^2/k_B$, and (d) $k_2/k_{\mathrm{tip}}=50$, $T=0.013k_{\mathrm{tip}}a^2/k_B$.

several values of k_2/k_{tip} at $T=0$ and at room temperature. $\langle F\rangle$ depends on both N and k_2/k_{tip} even at $T=0$ in Fig. 3(a), and it decreases with increasing k_2 contrary to the case of Fig. 2(b). For large values of k_2, $\langle F\rangle$ is reduced remarkably at a specific size, i.e., the magic size exists. In the case of $k_2=\infty$, the magic size is 9 since $0.887\times 9\simeq 8$.[22] It is seen in Fig. 3(a) that the magic size is increased slightly from $N=9$ with decreasing k_2 from ∞. The reduction of $\langle F\rangle$ at the size other than the magic size is also induced by suppression of the effective corrugation of the surface potential in the lattice-mismatched case, as seen in Fig. 1. At room temperature in Fig. 3(b), $\langle F\rangle$ is reduced remarkably for small values of k_2 similarly to the lattice-matched case in Fig. 2(b) and the opposite dependence on k_2 remains in a region of the tip size around the magic size. We have confirmed similar dramatic reduction of the averaged friction force at the magic size in other lattice-mismatched cases. In the case of $b=1.2a$, for example, the dramatic reduction of $\langle F\rangle$ was obtained at $N=5$, 10, and 15 for $k_2=\infty$.

Second, we study the origin of these behaviors of the averaged friction force. Figure 4 shows the time dependence of the tip position x_i, the position x_G of the center of mass, and the friction force F at room temperature for $b/a=1$ and $N=14$. In the case of $k_2=1$ in Figs. 5(a) and 5(b), each atom exhibits a coherent stick-slip motion inducing the stick-slip motion of x_G and the resultant saw-tooth behavior of F. On the other hand, in the case of $k_2=0$ in Figs. 4(c) and 4(d), each tip reveals jumps forth and back between the previous and final positions and exhibits incoherent stick-slip motion. As a result, it brings about wide variation of slip duration of x_G as pointed out by Maier *et al.*,[16] and F and the time-averaged friction force are reduced remarkably. Figure 5 shows the time dependence of the tip position x_i, the position x_G of the center of mass, and the friction force F at room temperature for $b/a=0.887$ and $N=9$. In the case of $k_2=1$ in Figs. 5(a) and 5(b), each atom shows a coherent stick-slip motion inducing the stick-slip motion of x_G and the resultant saw-tooth behavior of F. An intermediate jump which is induced by suppression of the effective corrugation of the surface potential can also be seen in Figs. 5(a) and 5(b). On the other hand, in the case of $k_2=50$ in Figs. 5(c) and 5(d), each tip shows a continuous motion with the large thermal fluctuation. The stick-slip motion of x_G disappears[4,5] and the averaged friction force $\langle F\rangle=0.0069$ approaches the viscous friction force, $m_{\mathrm{tip}}\mu v=0.0042$. This is caused by strong suppression of the effective corrugation of the surface potential.

Third, we study interatomic site correlation in the multiatomic contacts. Figure 6 presents (x_1-x_i) for $2\leq i\leq 14$ as a function of the position x_1 of the front atom for $b/a=1$. In the case of $k_2=1$ in Fig. 6(a) ($T=0.0026$) and Fig. 6(b) ($T=0.013$), the intervals between neighboring atoms are roughly kept to a. The slip positions of the front atom are distributed and the width of the distribution increases with temperature. In the case of $k_2=0$ in Fig. 6(c) ($T=0.0026$) and Fig. 6(d) ($T=0.013$), on the other hand, the intervals are not kept to a and the distribution of the slip position of the front

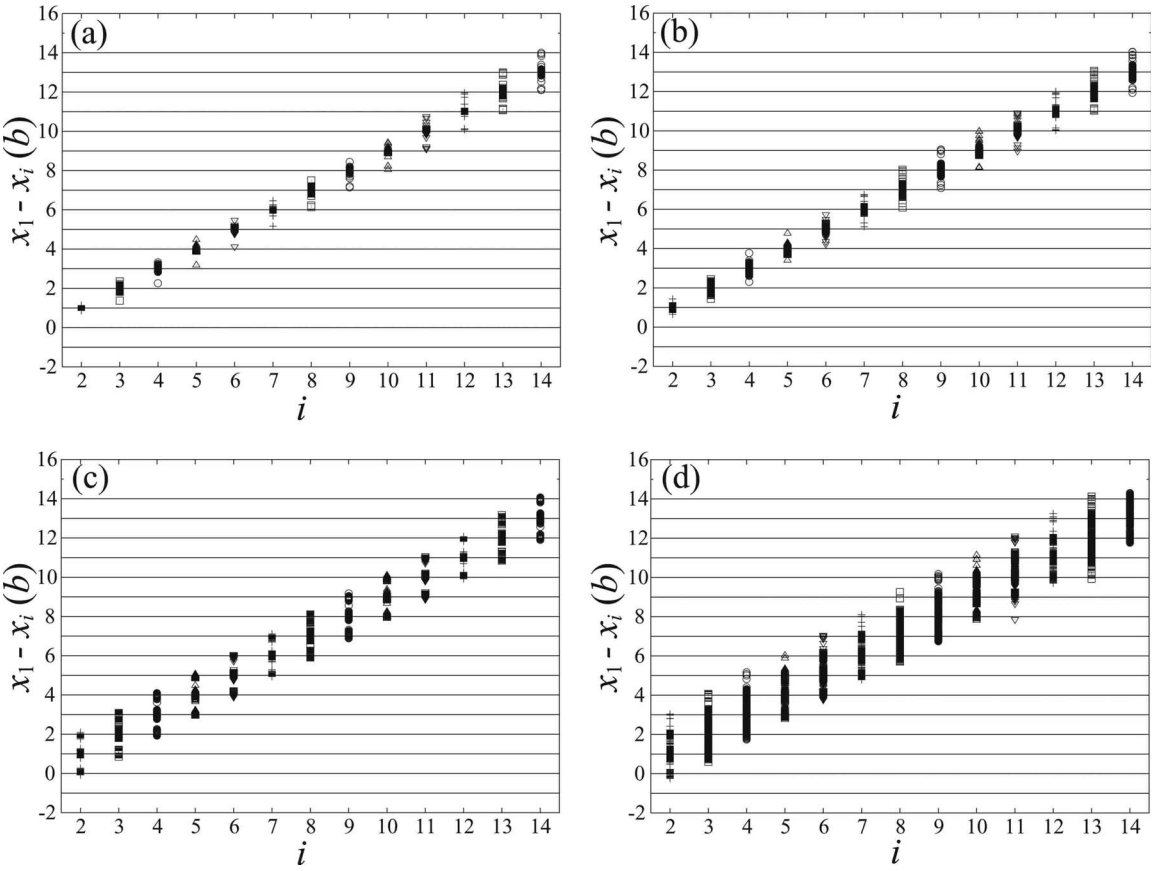

FIG. 8. (x_1-x_i) as a function of i at $N=14$ for $b/a=1$. (a) $k_2/k_{\rm tip}=1$, $T=0.0026k_{\rm tip}a^2/k_B$, (b) $k_2/k_{\rm tip}=1$, $T=0.013k_{\rm tip}a^2/k_B$, (c) $k_2/k_{\rm tip}=0$, $T=0.0026k_{\rm tip}a^2/k_B$, and (d) $k_2/k_{\rm tip}=0$, $T=0.013k_{\rm tip}a^2/k_B$.

atom have a larger width in comparison with the case of $k_2=1$. Figure 7 presents (x_1-x_i) for $2\leq i\leq 9$ as a function of the position x_1 for $b/a=0.887$. In the case of $k_2=1$ in Fig. 7(a) ($T=0.0026$) and Fig. 7(b) ($T=0.013$), the intervals between neighboring atoms are roughly kept to a but b since $8a\simeq 9b$. This means that the contact atoms take the commensurate positions with the substrate in the weak-coupling case. The slip positions of the front atom has a distribution and the width increases with temperature. In the case of $k_2=50$ in Fig. 7(c) ($T=0.0026$) and Fig. 7(d) ($T=0.013$), on the other hand, the intervals are kept to b but a, i.e., the incommensurate position with the substrate. The distribution of each slip position of the front atom has much larger width by reduction of the effective corrugation of the surface potential and the overlap between adjacent slips corresponds to nearly continuous motion.

To see clearly the site correlation among atoms in multiatomic contacts, (x_1-x_i) is replotted as a function of i. Figure 8 presents (x_1-x_i) for $2\leq i\leq 14$ as a function of i for $b/a=1$, corresponding to Fig. 6. In the case of $k_2=1$ in Fig. 8(a) ($T=0.0026$) and Fig. 8(b) ($T=0.013$), the average of (x_1-x_i) is well approximated as $\langle x_1-x_i\rangle\simeq(i-1)b$ and the dispersion of (x_1-x_i) increases monotonically with i. In the case of $k_2=0$ in Fig. 8(c) ($T=0.0026$) and Fig. 8(d) ($T=0.013$), the average of (x_1-x_i) can also be well approximated as $\langle x_1-x_i\rangle\simeq(i-1)b$, but the dispersion is large and almost independent of i. Figure 9 presents (x_1-x_i) for $2\leq i\leq 9$ as a function of i for $b/a=0.887$, corresponding to Fig. 7. In the case of $k_2=1$ in Fig. 7(a) ($T=0.0026$) and Fig. 7(b) ($T=0.013$), the average of (x_1-x_i) is well approximated as $\langle x_1-x_i\rangle\simeq(i-1)a$, i.e., the atoms take positions commensurate with the substrate. The dispersion of (x_1-x_i) increases monotonically with i. In the case of $k_2=50$, the average of (x_1-x_i) is well approximated as $\langle x_1-x_i\rangle\simeq(i-1)b$, i.e., the atoms take positions incommensurate with the substrate. The dispersion is small and is strongly suppressed in a short range. In Fig. 10, the standard deviations of (x_1-x_i) are plotted as a function of i for all the cases in Figs. 8 and 9. The suppression of the standard deviation of (x_1-x_i) means enhanced correlation between the first atom and the ith atom. In Fig. 10(a) for the lattice-matched case, the standard deviation is small compared to the lattice constant b of a tip and increases monotonically with i, in the case of $k_2=1$ corresponding to Figs. 6(a) and 6(b). This means that the site correlation is preserved over the multiatomic contact in a regime of the coherent stick-slip motion. On the other hand, the standard deviation is about $0.5b$ and almost independent of i, in the case of $k_2=0$ corresponding to Figs. 6(c) and 6(d). In a regime of the incoherent stick-slip motion, the site correlation is almost diminished independent of i. Meanwhile, in Fig. 10(b) for the lattice-mismatched case, the site correlation is preserved over the multiatomic contact and a monotonic weakening of the interatomic site correlation with i can be seen for both cases of the coherent stick-slip motion corresponding to Figs. 7(a) and 7(b) and the continuous motion corresponding to Figs. 7(c) and 7(d). As for the temperature

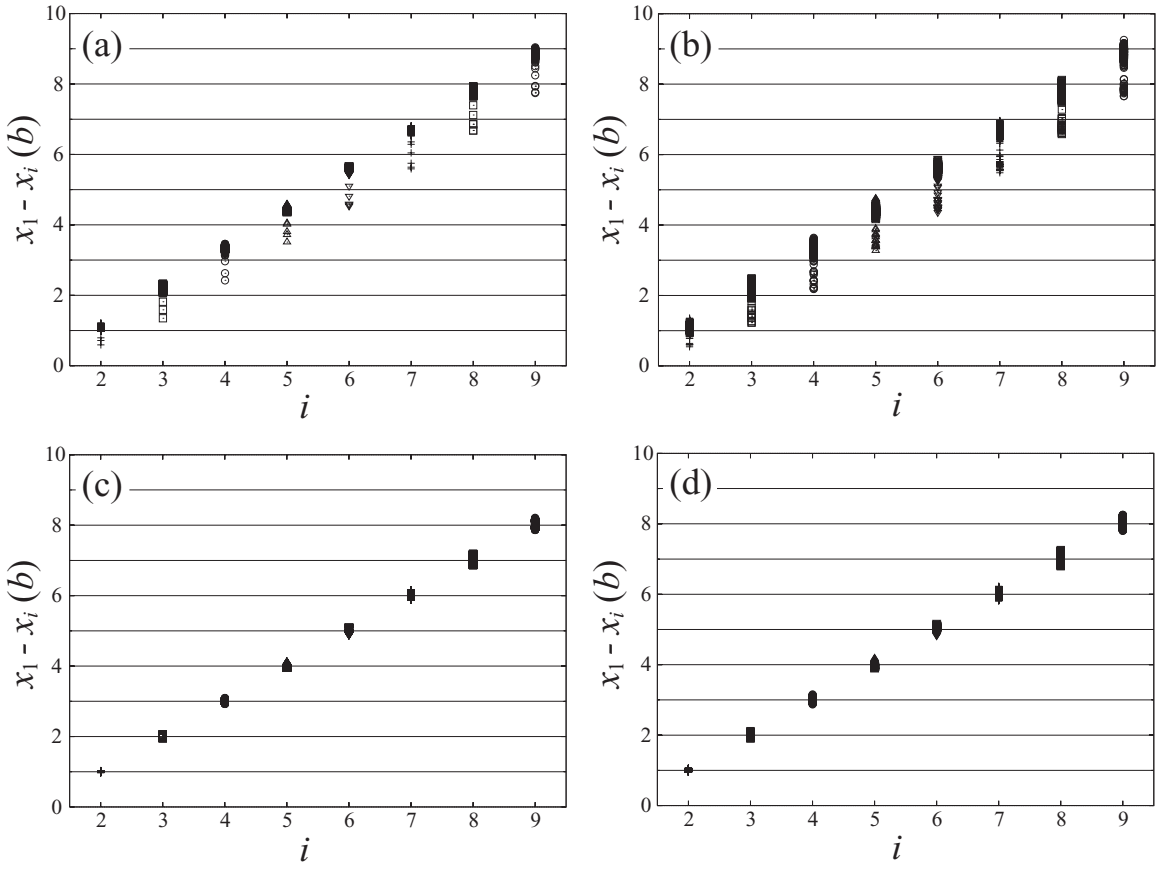

FIG. 9. (x_1-x_i) as a function of i at $N=9$ for $b/a=0.887$. (a) $k_2/k_{\mathrm{tip}}=1$, $T=0.0026k_{\mathrm{tip}}a^2/k_B$, (b) $k_2/k_{\mathrm{tip}}=1$, $T=0.013k_{\mathrm{tip}}a^2/k_B$, (c) $k_2/k_{\mathrm{tip}}=50$, $T=0.0026k_{\mathrm{tip}}a^2/k_B$, and (d) $k_2/k_{\mathrm{tip}}=50$, $T=0.013k_{\mathrm{tip}}a^2/k_B$.

dependence, the standard deviation is increased and the site correlation is weakened with increasing temperature for all the cases. Especially, the temperature effect is most efficient in the regime of the stick-slip motion for the lattice-mismatched case, since the effective corrugation of the substrate potential is suppressed.

Finally, we study the temperature dependence of $\langle F\rangle$. Figure 11(a) represents the temperature dependence of $\langle F\rangle$ for $b/a=1$ at $N=14$. As k_2 is decreased, $\langle F\rangle$ is decreased drastically with increasing temperature. Figure 11(b) represents the temperature dependence of $\langle F\rangle$ for $b/a=0.887$ at the magic size of $N=9$. For large values of k_2, $\langle F\rangle$ almost vanishes irrespective of temperature. However, for small values of k_2, large temperature dependence appears and $\langle F\rangle$ decreases remarkably as temperature increases.

IV. DISCUSSION AND CONCLUSION

The size effect in multiatomic contacts depends crucially on the coupling strength between atoms. In the strong-coupling case, both the lattice mismatch and the contact size influence strongly on the friction. Especially, the friction can be reduced nearly to zero at the magic size.[22] This is caused by suppression of the effective corrugation of the surface potential by taking incommensurate configuration with the substrate for the multiatomic contact, as seen in Figs. 7(c) and 7(d). In the weak-coupling case, on the other hand, the effect of thermal fluctuation is enhanced with increasing number of atoms and it results in remarkable reduction of the friction force irrespective of the lattice mismatch, as seen in Fig. 11.

Now, we will discuss the temperature T dependence of the averaged friction force in Fig. 11. In the case of $k_2=\infty$, it can be reduced to the single-tip results. Sang *et al.*[12] proposed the mechanism on the scanning velocity dependence of the friction force in the ramped creep regime, in which the thermally activated barrier-hopping fluctuations occur preferentially when the tip is close to slipping at the top of the barrier. The averaged friction force [a solid line in Fig. 11(a)] predicted by their theory agrees well with our simulated result for $k_2=\infty$. It suggests that the thermally activated barrier-hoppings occur in the vicinity of slipping points. In the opposite case of $k_2=0$ in Figs. 11(a) and 11(b), on the other hand, it can also be reduced to the single-tip results for the time averaged friction force if the temperature T is replaced by the effective temperature of NT. The random force f_i for the ith atom with mass of $m_i=m_{\mathrm{tip}}/N$ is proportional to $\sqrt{\mu m_i k_B T}$ and the temperature appears in Eq. (4) only through the random force f_i. The effective temperature for the multiatomic contact is proportional to f_i/m_i and hence it is increased to NT. This scaling of the effective temperature does not hold when there exists a coupling between atoms. The predicted averaged friction force at the effective temperature of NT is also drawn by broken lines in Figs. 11(a) and 11(b) and they also agree with our simulated results for $k_2=0$ in the region of low

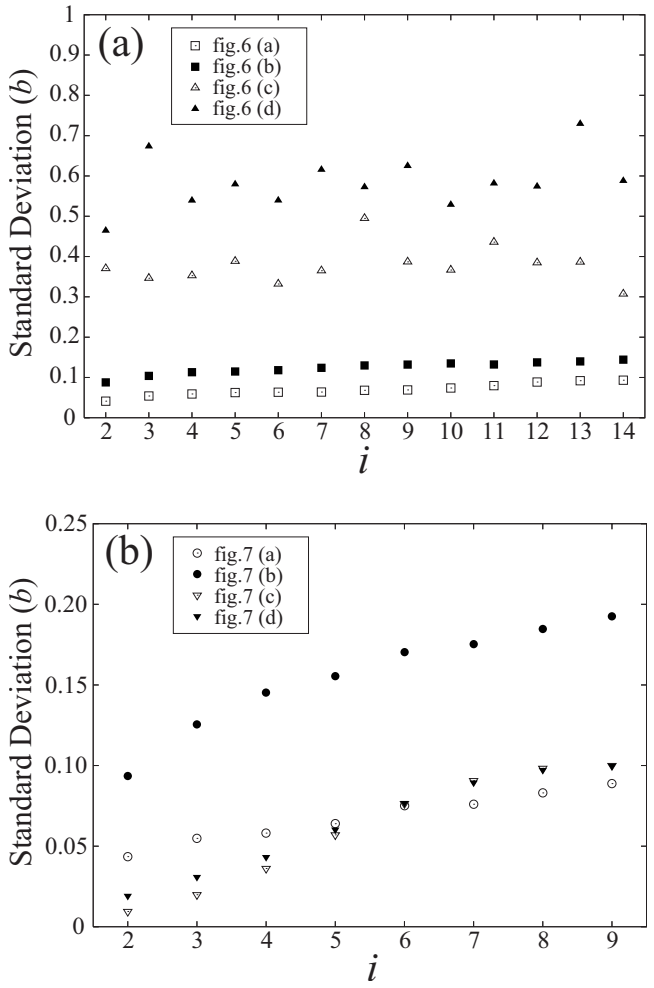

FIG. 10. The standard deviation of (x_1-x_i) as a function of i in two cases of (a) $N=14$ at $b/a=1$ and (b) $N=9$ at $b/a=0.887$. Four cases of $k_2/k_{\mathrm{tip}}=1$ at $T=0.0026k_{\mathrm{tip}}a^2/k_B$ and at $T=0.013k_{\mathrm{tip}}a^2/k_B$, $k_2/k_{\mathrm{tip}}=0$ at $T=0.0026k_{\mathrm{tip}}a^2/k_B$ and at $T=0.013k_{\mathrm{tip}}a^2/k_B$ are plotted in (a), corresponding to Figs. 6(a)–6(d), respectively. Four cases of $k_2/k_{\mathrm{tip}}=1$ at $T=0.0026k_{\mathrm{tip}}a^2/k_B$ and at $T=0.013$, $k_2/k_{\mathrm{tip}}=50$ at $T=0.0026k_{\mathrm{tip}}a^2/k_B$ and at $T=0.013k_{\mathrm{tip}}a^2/k_B$ are plotted in (b), corresponding to Figs. 7(a)–7(d), respectively.

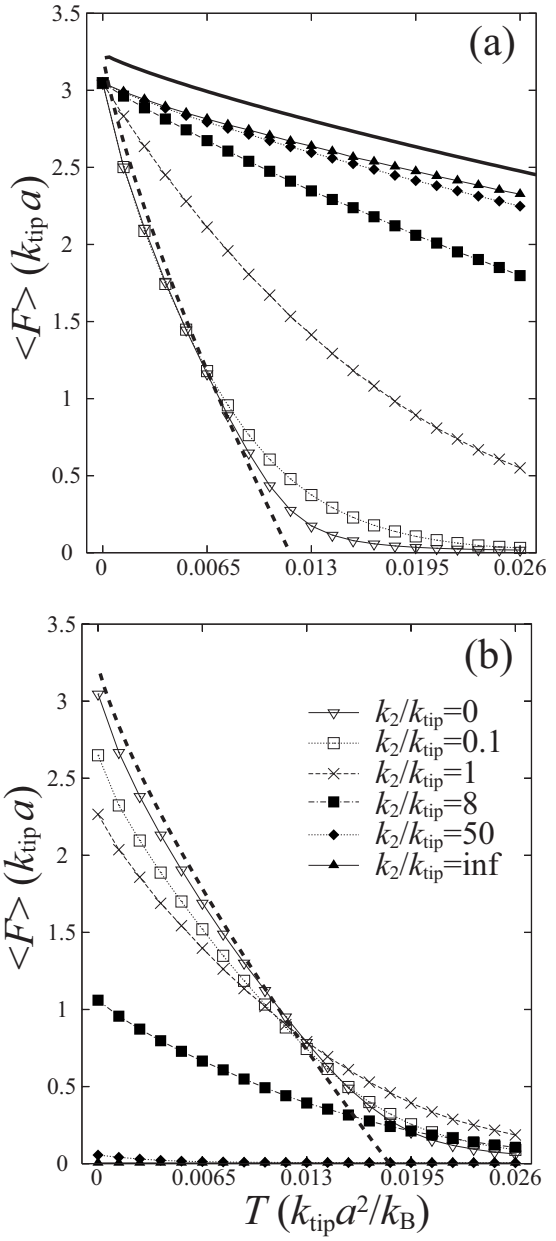

FIG. 11. The relation between the time-averaged friction force $\langle F\rangle$ and the temperature T for (a) the lattice-matched case of $b/a=1$ at $N=14$ and (b) the lattice-mismatched case of $b/a=0.887$ at $N=9$ for several values of k_2/k_{tip}. The solid line in (a) and the broken lines in (a) and (b) represent the predicted behavior in the ramped creep regime (Ref. 12) for $k_2=\infty$ and $k_2=0$, respectively.

temperatures. In Fig. 12, the time dependence of the tip position x_i, the position x_G of the center of mass, and the friction force F are shown at $T=0.0065$, for $a=b$, $k_2=0$, and $N=14$. Each tip exhibits a stick-slip motion although it is incoherent. The incoherence between slips does not affect the time-averaged friction force and hence the friction force can be predicted by the theory in the ramped creep regime.[12] The observed discrepancy at higher temperatures suggests that the assumption of the ramped creep regime cannot be satisfied at these substantially high effective temperatures. Each tip reveals jumps forth and back as seen in Fig. 4(c) and the barrier hoppings occur all over the stick point. Indeed, we observed significant reduction of the site correlation in multiatomic contact by increasing temperature in Fig. 8.

Next, we will discuss the k_2 dependence of the averaged friction force in Fig. 11. In the case of Fig. 11(a) for the lattice-matched case, the friction force is decreased monotonically with decreasing k_2 from that for $k_2=\infty$ to that for $k_2=0$. This is caused by the increase of the effective temperature as k_2 is decreased. On the other hand in Fig. 11(b) at the magic size for the lattice-mismatched case, the opposite k_2 dependence is seen in low temperatures. The dramatic decrease of the effective corrugation of the surface potential is induced by the incommensurate configuration of the multiatomic contact and it occurs only if the coupling between atoms is sufficiently strong. This corresponds to the opposite k_2 dependence of $\langle F\rangle$ in low temperatures in Fig. 11(b), i.e., $\langle F\rangle$ at the magic size decreases with the increasing coupling strength k_2 in low temperatures.

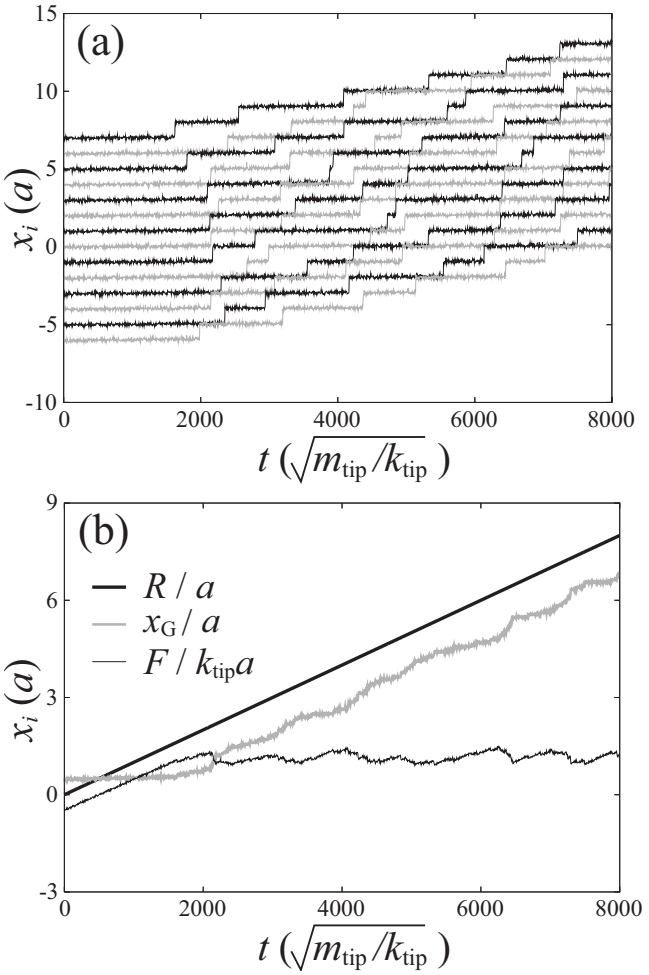

FIG. 12. The time t dependence of (a) x_i for $1 \leq i \leq 14$ and (b) x_G and F with $R=vt$ for $k_2=0$. Here, $N=14$, $b/a=1$, and $T=0.0065k_{\rm tip}a^2/k_B$.

Finally, we will comment on the magnitude of the calculated average friction force $\langle F \rangle$. In the single-atomic tip case of $k_2=\infty$, the average friction force becomes approximately 1.7 nN at room temperature in Fig. 11. We assumed the effective spring constant $k_{\rm tip}$ of 1.2 N/m, the lattice constant of the substrate a of 0.52 nm, the sliding velocity v of 0.328 μm/s, and the surface-potential corrugation U of 1.1 eV. For these situations, the average friction force has been measured and the value is approximately 1.3 nN.[4] The slight discrepancy may be caused by the multiatomic contact.

In summary, we studied the multiatomic contact effect on the atomic friction of a friction force microscope at a finite temperature using the dynamical simulation of the Frenkel-Kontrova-Tomlinson model with a finite contact size. The friction force depends crucially on both the lattice mismatch between the tip and the sample surface and the strength of coupling between atoms. In the case of strong coupling, the friction force depends strongly on both the lattice mismatch and the tip size: there exists a magic size at which the friction force is reduced dramatically due to suppression of the effective corrugation of the surface potential to drive the tip. In the case of weak coupling, the friction force is reduced more largely with increasing temperature as the contact size increases, irrespective of the lattice mismatch. This is caused by the enhanced thermal fluctuation of the multiatomic contact.

ACKNOWLEDGMENTS

The authors acknowledge H. Iiduka for his kind help with numerical calculation. This work was supported by Grant No. 18540313 in Aid for Scientific Research from the Ministry of Education, Culture, Sports, Science, and Technology of Japan.

*natori@ee.uec.ac.jp
†junj@ee.uec.ac.jp; http://www.natori.ee.uec.ac.jp/junj/

[1] C. M. Mate, G. M. McClelland, R. Erlandsson, and S. Chiang, Phys. Rev. Lett. **59**, 1942 (1987).
[2] A. Socoliuc, E. Gnecco, S. Maier, O. Pfeiffer, A. Baratoff, R. Bennewitz, and E. Meyer, Science **313**, 207 (2006).
[3] G. A. Tomlinson, Philos. Mag. **7**, 905 (1929).
[4] E. Riedo, E. Gnecco, R. Bennewitz, E. Meyer, and H. Brune, Phys. Rev. Lett. **91**, 084502 (2003).
[5] A. Socoliuc, R. Bennewitz, E. Gnecco, and E. Meyer, Phys. Rev. Lett. **92**, 134301 (2004).
[6] Y. Hoshi, T. Kawagishi, and H. Kawakatsu, Jpn. J. Appl. Phys., Part 1 **39**, 3804 (2000).
[7] K. L. Johnson and J. Woodhouse, Tribol. Lett. **5**, 155 (1998).
[8] C. Fusco and A. Fasolino, Phys. Rev. B **71**, 045413 (2005).
[9] J. Nakamura, S. Wakunami, and A. Natori, Phys. Rev. B **72**, 235415 (2005).
[10] S. N. Medyanik, W. K. Liu, I. H. Sung, and R. W. Carpick, Phys. Rev. Lett. **97**, 136106 (2006).
[11] E. Gnecco, R. Bennewitz, T. Gyalog, C. Loppacher, M. Bammerlin, E. Meyer, and H.-J. Güntherodt, Phys. Rev. Lett. **84**, 1172 (2000).
[12] Y. Sang, M. Dube, and M. Grant, Phys. Rev. Lett. **87**, 174301 (2001).
[13] P. Reimann and M. Evstigneev, Phys. Rev. Lett. **93**, 230802 (2004).
[14] M. Evstigneev and P. Reimann, Phys. Rev. B **73**, 113401 (2006).
[15] M. Igarashi, J. Nakamura, and A. Natori, Jpn. J. Appl. Phys., Part 1 **46**, 5591 (2007).
[16] S. Maier, Y. Sang, T. Filleter, M. Grant, R. Bennewitz, E. Gnecco, and E. Meyer, Phys. Rev. B **72**, 245418 (2005).
[17] S. Y. Krylov, J. A. Dijksman, W. A. van Loo, and J. W. M. Frenken, Phys. Rev. Lett. **97**, 166103 (2006).
[18] Y. Braiman, F. Family, and H. G. E. Hentschel, Phys. Rev. B **55**, 5491 (1997).
[19] H. G. E. Hentschel, F. Family, and Y. Braiman, Phys. Rev. Lett. **83**, 104 (1999).

[20] M. Weiss and F. J. Elmer, Phys. Rev. B **53**, 7539 (1996).
[21] M. Weiss and F. J. Elmer, Z. Phys. B: Condens. Matter **104**, 55 (1997).
[22] K. Ohno, T. Nitta, J. Nakamura, and A. Natori, J. Vac. Sci. Technol. B **22**, 2026 (2004).
[23] S. Y. Krylov, Phys. Rev. Lett. **83**, 4602 (1999).
[24] M. P. Allen and D. J. Tildesley, *Computer Simulations of Liquids* (Clarendon, Oxford, 1990).